ELSEVIER

Surface melting of superheated crystals. Atomistic simulation study

A.Yu. Kuksin [a,b], G.E. Norman [a,b], V.V. Stegailov [a,b,*], A.V. Yanilkin [a,b]

[a] *Institute for High Energy Densities JIHT RAS, Izhorskaya st. 13/19, Moscow 125412, Russia*
[b] *Department of Molecular and Biological Physics, Moscow Institute of Physics and Technology, Dolgoprudny 141700, Russia*

Available online 28 February 2007

Abstract

Melting front velocity dependencies on temperature are calculated using the molecular-dynamics method for the EAM models of Al and Fe as well as for the Lennard-Jones system. Different surface orientations are considered. It is shown that the Broughton–Gilmer–Jackson theory of the collision-limited growth can describe the results obtained. The isochoric bulk solid melting and decay under ultrafast heating is simulated for mono- and polycrystalline models.
© 2007 Elsevier B.V. All rights reserved.

Keywords: Melting; Crystal-liquid interface; Superheating; Molecular dynamics

1. Introduction

Melting mechanisms and kinetics is a long-standing topic of interest for atomistic simulation. Since the pioneering work of Broughton and Woodcock [1] where the premelting effects on the (100) Lennard-Jones crystal surface were studied, the theory of equilibrium surface properties near the bulk melting point has been well established (e.g., see the review [2]). In a number of works the kinetics of the crystal–liquid transition was studied primarily with regard to the solidification kinetics (e.g., [3–5] and references therein). Less attention was addressed to the melting kinetics itself: e.g., in [6] the velocity of the melting front propagation was calculated at different temperatures, and the similarity between the open surface melting and the grain boundary melting was shown.

A relatively larger attention to the solidification kinetics is caused by its obvious technological importance for crystal growth applications [7]. At the same time the atomistic-level melting kinetics and the solid superheating effects are usually considered to be negligible for the experiments where melting takes place. Local melting propagates from the open surfaces, grain boundaries and defects of the crystal structure. Taking into account the polycrystalline structure of usual solids it is accepted that the local melting of the substance takes place as soon as the local temperature equals the equilibrium melting temperature.

However under conditions of recent experiments connected with ultrafast high energy deposition at the nanosecond time scale (electrical explosions of wires, laser heating, shock waves) it is expected that the superheated solid phase could be one of the transient states during the solid phase evolution [8] and the melting kinetics is to be taken into account.

In Section 2 of the paper we describe the results on melting front velocity dependencies on temperature for the Lennard-Jones (LJ) solid and Al and Fe modeled by EAM potentials and make some general conclusions on the melting kinetics mechanisms. In Section 3 we compare the results of the atomistic simulation of the isochoric bulk solid melting and decay under ultrafast heating for monocrystalline and polycrystalline solids. We use these results in order to illustrate the possibility of solid superheating under special conditions.

2. Melting front propagation kinetics

For molecular dynamics simulation of the melting front propagation from the free surface of a superheated crystal we use simulation boxes that are elongated in the z direction and have square cross-section in the x–y plane. Initially the simulation box is filled by atoms on the crystal lattice with the specific orientations (100), (110) or (111). At each temperature the lattice constant value is chosen from the zero stress condition.

* Corresponding author at: Institute for High Energy Densities JIHT RAS, Izhorskaya st. 13/19, Moscow 125412, Russia.

E-mail address: stegailov@ihed.ras.ru (V.V. Stegailov).
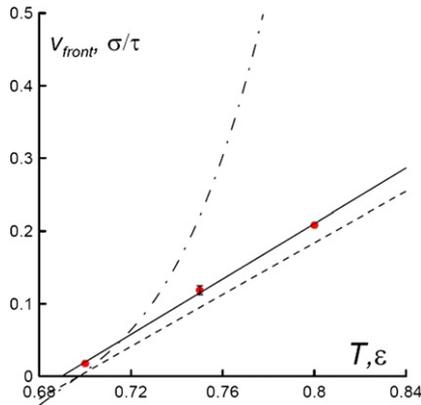
Fig. 1. The dependence of the melting front propagation velocity v_{front} on the maintained temperature T for the LJ crystal (100) surface. The solid line is a linear fit through the points obtained. The dashed-dotted and dashed lines correspond to the results from [4] for the 1 "transient" and 2 "steady state" regimes, respectively.

Fig. 2. Results for the (001), (110) and (111) surface orientations for f.c.c. Al. The zero values of velocities for the (111) orientation correspond to the surface superheating, the non-zero values at the same T correspond to the initial configuration with the liquid layer at the surface (see text).

Fig. 3. Results for b.c.c. Fe. Solid lines correspond to the results of [5] for similar EAM model of Fe [10] (potential 2): the blue line—(001), the green line—(110), red line—(111). The dotted line is the linear fit over the data obtained (including all orientations) that gives $\mu = 74.7$ cm/s/K. (For interpretation of the references to color in this figure legend, the reader is referred to the web version of this article.)

In order to prepare the initial configuration the crystal lattice in the simulation box is equilibrated in 3D periodic boundary conditions. The given value of temperature $T > T_m$ (T_m—the equilibrium melting temperature) is maintained in the whole system by the Langevin thermostat. After equilibration a rectangular layer of the lattice is cut away. The width of the removed piece is slightly larger than two potential cut-off radii, therefore the system remains effectively in the 2D periodic boundary conditions with 2 free surfaces in the z direction. As soon as two free surfaces have been formed in the system the melting front propagation starts. The degree of the crystal-to-liquid phase transformation during the melting front propagation from the open surface to the bulk is shown by the static structure factor profile [6]. The system size used for production runs was chosen to be $20 \times 20 \times 60$ f.c.c. (for LJ, Al) or b.c.c. (Fe) unit cells (no significant difference was found for systems sizes $12 \times 12 \times 60$ and $36 \times 36 \times 60$ unit cells). The potential models considered in this work are the Lennard-Jones 12-6 potential (with the cut-off at 7.0σ) and the EAM models for Al [9] and Fe [10] (potential 4). Simulation were performed using the molecular dynamics code LAMMPS [11]. Timestep equals 1 fs for the Al and Fe models, and 0.004τ for the LJ model ($\tau = (m\sigma^2/\epsilon)$ is the LJ unit of time). The Langevin thermostat relaxation time where varied in the range 1–10 ps and no dependence of the results on this parameter was found.

The results of the melting front velocity v_{front} calculation for the (100) free surface of the f.c.c. LJ crystal is presented on Fig. 1. These results are compared with [4]. In [4] the authors considered a two-phase model that did not contain free surfaces (i.e. crystal/liquid–vacuum interfaces), but initially was prepared as the adjacent liquid and crystal parts. The crystal–liquid interface motion velocity was studied in the smaller undercooling/superheating region $T = \pm 0.06\epsilon$. The authors distinguished two stages of the crystal–liquid interface motion (1—transient, 2—steady state, see Fig. 1). The results obtained in this work are in a good agreement with the 2 regime results. The small discrepancy of the results is attributed to the difference in the potential cut-off distances (2.5σ in [4]).

The $v_{\text{front}}(T)$ dependencies on temperature were calculated for (001), (110) and (111) surface orientations of Al and Fe crystal models (shown on Figs. 2 and 3). The possibility of superheating of the close-packed Al surface is observed as expected for f.c.c. crystals [2]. In the case of small superheatings $T - T_m < 50$ K the close-packed surface remains stable. In order to initiate melting the surface liquid layer has been formed artificially. In this case the melting front propagation starts without the barrier caused by the high close-packed surface stability.

The melting front velocity dependencies rise in a similar way for all three surface orientations considered for Al and Fe. This fact does not agree with the results (for several metals) that show the dependence of the kinetic coefficient μ on the surface orientation: $\mu_{(100)} > \mu_{(110)} \sim \mu_{(111)}$, where μ is the proportionality constant $v_{\text{front}} = \mu(T - T_m)$ [3,5]. However the results presented show that the melting velocities in the [001] direction is slightly higher than the velocities in [110] and [111] directions.
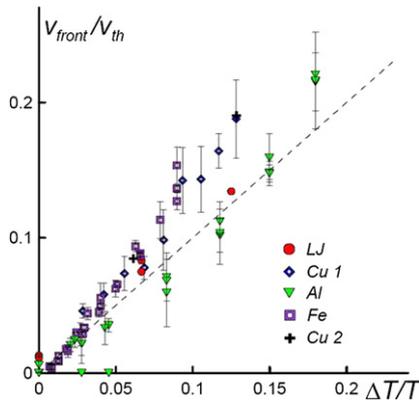
Fig. 4. The $v_{\text{front}}(T)$ dependence in the dimensionless parameters $v_{\text{front}}/v_{\text{th}}$ and $\Delta T/T$. The results are given for the (100), (110) and (111) surface orientations simultaneously. The results for Cu (1—[12], 2—[6]) obtained via similar approach. The dotted line corresponds to the slope of unity.

It is interesting to compare our results for Fe with the results of [5] where a similar potential [10] (potential 2) was used. Our results do not show the difference in the kinetic coefficients for different orientations. The slope of the obtained $v_{\text{front}}(T)$ dependence $\mu = 74.7$ cm/s/K is ~1.5–2 times larger than those obtained by Sun and coauthors. However, at small values of superheating ($T < 1810$ K) the results of this work become close to those from [5].

According to the work [10] the difference between the potential 2 and potential 4 developed in that work are very small. Potential 4 has an advantage over potential 2 being fitted to the experimental structure factor of the liquid iron. Potential 4 provides more accurate values of the surface energy in bcc iron at $T = 0$ K, latent heat of melting and volume change than does potential 2, although slightly worse values for the melting temperature and the activation energy for self-diffusion in bcc iron. The authors [10] give the following melting temperatures for these potentials: 2—1772 K; 4—1753 K. The $v_{\text{front}}(T)$ dependence obtained in this work gives the estimate of the equilibrium melting temperature 1785 ± 5 K for potential 4.

Comparison with the BGJ theory. The Broughton–Gilmer–Jackson theory was developed in order to describe the collision-limited growth kinetics of crystallization. In the limit of small undercooling ΔT the crystallization growth rate changes as $v_{\text{front}} \sim v_{\text{th}}\Delta T/T$, where $v_{\text{th}} = (3k_B T/m)^{1/2}$ is the thermal velocity and $\Delta T = T - T_m$ [14]. The BGJ theory of crystallization can be transferred to the case of melting. On Fig. 4 the results obtained for different systems are presented in the dimensionless variables $v_{\text{front}}/v_{\text{th}}$ and $\Delta T/T$. All the dependencies have the close values of slope (with some deviation for Al) that is close to unity. This is the evidence that the melting kinetics of monoatomic solids is a collision-limited process and its rate can be estimated as $v_{\text{th}}\Delta T/T$ for superheatings up to $\Delta T/T = 0.2$.

3. Melting of mono- and polycrystalline solids under ultrafast isochoric heating

The molecular-dynamics model for the simulation of the bulk melting uses a cubic simulation box in 3D periodic boundary conditions. The EAM potential model for Cu [13] was used.
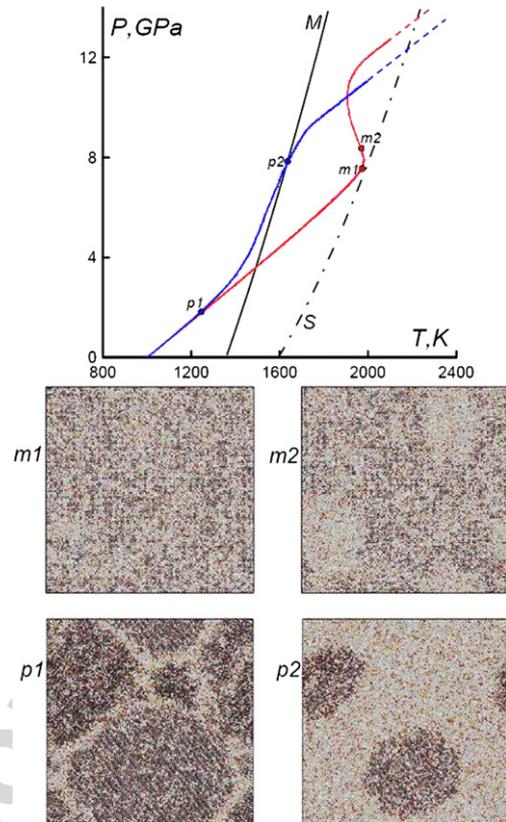
Fig. 5. The illustration on the pressure–temperature plot. M is the melting line of copper well reproduced in the EAM model, S is the crystal stability boundary. Cross-sections of the atomic structure in the simulation box is shown (the lighter the atom's color the less ordered is its local neighborhood): $p1$ and $p2$—polycrystalline solid before grain-boundary melting starts and after ~250 ps, $m1$—strongly superheated lattice, $m2$—growth of the homogeneously formed liquid nuclei. The system size is ~0.5 millions of atoms. (For interpretation of the references to color in this figure legend, the reader is referred to the web version of this article.)

The initial state corresponds to the equilibrated zero stress single crystal or the polycrystalline structure. The latter was created by dividing the simulation box into a number of Voronoi polyhedra and filling them with random orientations of the f.c.c. lattice (removing the overlapping atoms). In both cases the system was heated using Langevin thermostat, which temperature was assigned to increase at 2.3 K/ps (see Fig. 5). We treat two cases considered as the limiting cases that describe the polycrystalline solid with nanosized grains and large grains of (say) micrometer size. The finite velocity of the melting front propagation from the grain boundaries can result in the superheating of the bulk solid limited by the homogeneous nucleation near the stability boundary [12]. This effect vanishes as the grain size decreases. The maximum achievable superheating can also depend on the solid thermal conductivity because of heat fluxes to the fusion region (electron thermal conductivity is not considered in this model).

References

[1] J.Q. Broughton, L.V. Woodcock, J. Phys. C: Solid State Phys. 11 (1978) 2743.

[2] U. Tartaglino, T. Zykova-Timan, F. Ercolessi, E. Tosatti, Phys. Reports 411 (2005) 291.

[3] F. Celestini, J.-M. Debierre, Phys. Rev. E 65 (2002) 41605.

[4] H.L. Tepper, W.J. Briels, J. Chem. Phys. 115 (2001) 9434.

[5] D.Y. Sun, M. Asta, J.J. Hoyt, Phys. Rev. B 69 (2004) 174103.

[6] J.F. Lutsko, D. Wolf, S.R. Phillpot, S. Yip, Phys. Rev. B 40 (1989) 2841.

[7] J.J. Hoyt, M. Asta, A. Karma, Mat. Sci. Eng. R 61 (2003) 121.

[8] G.E. Norman, V.V. Stegailov, A.A. Valuev, Contrib. Plasma Phys. 43 (2003) 384.

[9] Y. Mishin, D. Farkas, M.J. Mehl, D.A. Papaconstantopoulos, Phys. Rev. B 59 (1999) 3393.

[10] M.I. Mendelev, S. Han, D.J. Srolovitz, G.J. Ackland, D.Y. Sun, M. Asta, Phil. Mag. 83 (1999) 3977.

[11] S.J. Plimpton, J. Comp. Phys. 117 (1995) 1.

[12] V.V. Stegailov, Comput. Phys. Comm. 169 (2005) 247.

[13] Y. Mishin, M.J. Mehl, D.A. Papaconstantopoulos, A.F. Voter, J.D. Kress, Phys. Rev. B 63 (2001) 224106.

[14] K.A. Jackson, Kinetic Processes: Crystal Growth, Diffusion, and Phase Transitions in Materials, Wiley-VCH, Weinheim, 2004, p. 409.